THE JOURNAL OF PHYSICAL CHEMISTRY A

Article

pubs.acs.org/JPCA

Quantum Dynamics Study of the F + CH_4 → HF + CH_3 Reaction on an Ab Initio Potential Energy Surface

Dunyou Wang*

College of Physics and Electronics, Shandong Normal University, 88 East Wenhua Road, Jinan 250014, People's Republic of China

Gábor Czakó†

Laboratory of Molecular Structure and Dynamics, Institute of Chemistry, Eötvös University, H-1518 Budapest 112, P.O. Box 32, Hungary

Supporting Information

ABSTRACT: A quantum reactive dynamics, four degree-of-freedom, time-dependent wavepacket method is applied to study the F + CH_4 → HF + CH_3 reaction using a slightly modified version of the ab initio potential energy surface of Czakó et al. [*J. Chem. Phys.* **2009**, *130*, 084301]. A common resonance peak is found on all initial state-selected reaction probabilities close to the reaction threshold. The resonance also survives the averaging of partial waves and shows up in the integral cross section just after the threshold energy, in agreement with experiment. This early- barrier polyatomic reaction is more enhanced by the translational motion than the vibrational motion for energies below 0.38 eV; however, the reverse is true for energies higher than 0.38 eV. The vibrational excitation of the CH stretching mode enhances the reactivity, whereas the excitation of the umbrella mode of CH_4 hinders the reactivity. The calculated thermal rate constants are in good agreement with one direct experimental measurement.

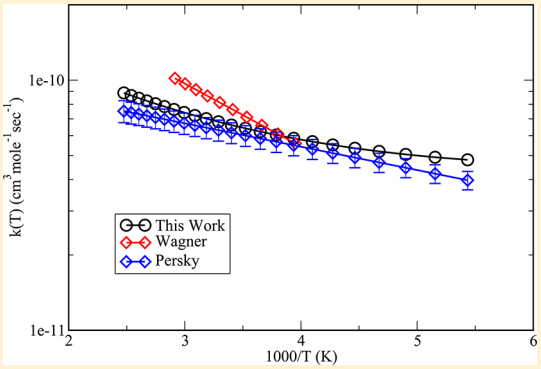

1. INTRODUCTION

A lot of attention has been paid to the F + CH_4 reaction as it serves as one of the prototypes to understand the driving force for polyatomic reaction dynamics. For the atom−diatom reactions, the Polanyi rules[1] state that for an early saddle point in the entrance channel of the reaction, translational motion plays a more important role in the reactivity than the vibrational excitations, and for a late transition state in the product channel, the reverse is true. However, we are not sure whether these rules are still valid for the reaction systems with more than three atoms, especially when van der Waals (vdW) wells show up on the multidimensional potential energy surfaces (PESs), which make the scenario more complicated to distinguish which force drives the reaction. For example, the full-dimensional ab initio potential energy surface of the F + CH_4 reaction[2] has an early saddle point located in the reactant channel, a van der Waals valley in the entrance channel, and an additional relatively deep vdW minimum in the product valley. The complex feature of this PES makes it difficult to predict which motion drives the reaction.

A more extreme case is the H_3^+ + H_2 reaction system because the potential energy surface[3] has 10 stationary points, that is, 1 global minimum and nine saddle points (three in the reactant channel and the other six in the product channel). Therefore, it is even more difficult to tell if an early saddle point drives the reaction or a late barrier does. Indeed, the seven degree-of-freedom (7DOF) quantum reaction dynamics calculation[4] for the isotopic reaction, H_2D^+ + H_2 → H_3^+ + HD, shows that the stretching motion of H^+−HD only has a small effect on the reaction probability; the vibrational excitation of HD in H_2D^+ hinders the reactivity. By contrast, rotational excitation of H^+−HD greatly enhances the reactivity by a factor of about 2−3 for high rotational states relative to the reactivity of the ground-state reaction. To our knowledge, this is the first time that we observed that the rotational excitations dominate the polyatomic reactivity not the vibrational and translational energy.

We know that excited polyatomic vibrational motions can have profound effects on the chemical reactivity; however, not all vibrational modes exert the same effects on reactivity. More interestingly, in 2007, Liu et al.[5] found that the translational energy has a larger effect on the reactivity of the late-barrier Cl + CHD_3 reaction than the excitation of the reactant CH stretching mode, which contradicts the Polanyi rules. In 2012, a

Special Issue: Joel M. Bowman Festschrift

Received: January 17, 2013
Revised: March 16, 2013
Published: April 25, 2013

   dx.doi.org/10.1021/jp4005778 | *J. Phys. Chem. A* 2013, 117, 7124−7130

6DOF quantum study[6] on the Cl + CH_4 reaction showed that at very low scattering energies, the translational energy indeed drives the reaction more than the vibrational energy for this late-barrier reaction. Then, a 7DOF quantum dynamics study[7] on Cl + CHD_3 showed that the Polanyi rules hold for the Cl + CHD_3 reaction, except at very low collision energies. Both quantum dynamics studies were carried out on the same accurate ab initio PES.[9] This theoretical work inspired an experimental reinvestigation, which found that probing all of the rotational states of the $CD_3(\nu = 0)$ products bring theory and experiment into agreement.[8] It is clear that the detailed dynamics of which energy forms drive the polyatomic reactions has not been well-understood, and both experimental and theoretical work need to be combined to understand the fundamental mechanism and rules of the polyatomic reactions.

The F + CH_4 reaction has been studied extensively both experimentally[10−21] and theoretically[2,22−32] because it plays an important role in atmospheric chemistry and has become a benchmark system to study polyatomic reactivity. Experimental studies by Liu and co-workers[18] on the title reaction revealed resonance signatures near the reaction threshold. In addition, the resonances also appeared in the F + CHD_3 reaction, and the experimental study concluded that the resonances can survive the averaging over impact parameters and show up in the integral cross sections in favorable cases.[19] Furthermore, another experiment[33] on the CH stretching excitation in this early-barrier F + CHD_3 reaction showed that one quantum excitation of the CH stretch mode of CHD_3 slows down the reaction rate and favors the DF + CHD_2 products. This unexpected experimental finding was recently explained by quasiclassical trajectory (QCT) calculations showing that a long-range stereodynamical interaction induced by the CH stretching excitation steers the slow F atom to one of the CD bonds, thereby promoting the D-abstraction channel at low collision energies.[31,32] The recent experimental study also by Liu et al.[34] on F + CH_4 found that the antisymmetric stretch of CH_4 prohibits the CH bond rupture.

Several quantum reaction dynamics studies have been performed on the title reaction.[27−30] Han et al. performed a 5DOF SVRT model calculation[27] using two different PESs constructed based on the analytical form proposed by Jordan and Gilbert for the H + CH_4 reaction.[35] Resonance was observed on one of the PESs near the threshold but disappeared for a partial wave J greater than 30. No rate coefficients were calculated from this study. A 3DOF time-independent calculation[28] and a 5DOF SVRT study[29] were carried out on the PES-2006 F + CH_4 surface developed by the Espinosa-Garcia group.[36] In the 5DOF study,[29] a single resonance peak was found in the reaction probabilities for $J \leq 55$. Rate constants were also reported in the 5DOF study; the results showed that over the temperature range of 180−400 K, the 5DOF results underestimated and overestimated the experimental results at low and high temperatures by factors of 1.17 and 1.21, respectively. Clary and co-workers carried out a 2DOF quantum study[30] on the isotopic reaction of F + CHD_3 to study the reactive resonance and cross sections.

In the present study, we carry out reduced-dimensional, 4DOF quantum reaction dynamics computations to study the title reaction on a modified ab initio full-dimensional PES.[2] The purpose here is three-fold, (1) exploring the resonance features discovered in the experimental studies,[17,18] (2) theoretically investigating early barrier effects on the reaction dynamics, and (3) comparing our computed thermal rate constants with the available experimental results.[20,37]

We perform our quantum reactive dynamics on the title reaction using an ab initio full-dimensional PES. This is the first quantum reaction dynamics calculation on this PES. The original PES, reported in ref 2, was based on 19384 high-quality ab initio energies describing the complex region FCH_4 (12384) and the fragment channels, F + CH_4 (2000), HF + CH_3 (2000), CH_2F + H_2 (2000), and CH_3F + H (1000), where the number of data points is given in parentheses. This PES has been used in a couple of QCT studies.[2,31,32] The agreement between the computed and measured product distributions, for example, HF(ν,j) rovibrational populations,[2] was impressive; however, the QCT results are sensitive to the binning technique. Furthermore, tunneling may also have a significant effect on the dynamics, especially at low collision energies, which adds to our motivation to carry out quantum dynamics computations for the title reaction. For the present quantum study, we have further improved the short-range and three-body regions of the PES in order to avoid any pathological behavior of the wave packet. We have added 1381 new data points to the original data set, (a) 1200 UCCSD(T)/aug-cc-pVTZ energy points corresponding to the CH_3 + F + H configurations and (b) 181 very high energy points in the short-range region, where both CH and HF distances are short. We obtained the analytical PES by a weighted linear least-squares fit to the combined 20765 energy points using a six-order polynomial basis of Morse-like variables that is explicitly invariant under the permutations of like atoms. The parameters used during the fit are the same as those in ref 2. All of the properties of the original and modified PESs are very similar, as shown in Table S1 of the Supporting Information, except that the revised PES has an improved short-range behavior and dissociates properly to CH_3 + H + F.

This paper is organized as follows. In section 2, we briefly describe the reduced-dimensional, 4DOF quantum reactive dynamics approach for this reaction system. Section 3 presents the initial state-selected reaction probabilities, integral cross sections, cumulative reaction probability, and rate coefficients, as well as the explanation and discussion of the computed results. Conclusions are given in section 4.

2. THEORETICAL METHODS

A. 4DOF Approach. In this 4DOF quantum dynamics approach, we treat this reaction as an atom−triatom system, F + HCX, as shown in Figure 1, where three H atoms are treated as one pseudoatom, X, with its mass located at the center of mass of the three nonreactive H atoms. Thus, the 4DOF includes the CX vibrational motion (r), which approximately represents the umbrella motion of CH_3 with CH bond lengths fixed at the saddle point values, the bond-breaking motion (ρ), and the translational motion (R); because at the reaction saddle point the C−H−F is not linear, but slightly bent, we also consider one bending motion (as shown as the γ DOF in Figure 1). Thus, the interaction potential for this 4DOF approach only has four variables, R, ρ, r, and γ, while θ and ϕ are fixed at the transition-state geometry.

The 4DOF Hamiltonian in reactant Jacobi coordinates, as shown in Figure 1, can be written as

dx.doi.org/10.1021/jp4005778 | J. Phys. Chem. A 2013, 117, 7124−7130

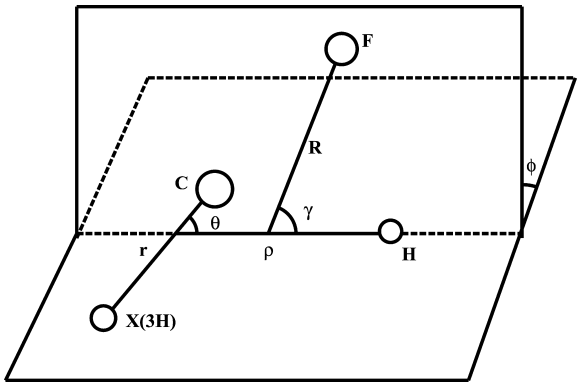

Figure 1. Reactant Jacobi coordinates for F + CH_4. In the 4DOF model, the active coordinates are R, ρ, r, and γ, whereas θ and ϕ are fixed at their saddle point values.

$$\hat{H} = -\frac{\hbar^2}{2\mu}\frac{\partial^2}{\partial R^2} + \frac{(\mathbf{J}-\mathbf{j})^2}{2\mu R^2} + h_r(r) + h_\rho(\rho) + \frac{\mathbf{j}^2}{2\mu_\rho r_\rho^2} + V_{4D}(R, r, \rho, \gamma) \quad (1)$$

Here, the first term is the translational energy of the reaction system, μ is the reduced mass of the system, and R is the distance between the center of mass of CHX and the F atom. The r is the bond length from the X(3H) pseudoatom to C, ρ is the distance from the center of mass of CX to H, γ is the Jacobi angle formed by ρ and R, $\mathbf{J}$ is the total angular momentum operator, and $\mathbf{j}$ is the rotational angular momentum operator of H−CX.

The vibrational reference Hamiltonians $h_r(r)$ and $h_\rho(\rho)$ are defined as

$$h_r(r) = -\frac{\hbar^2}{2\mu_r}\frac{\partial^2}{\partial r^2} + V_{1D}(r) \quad (2a)$$

$$h_\rho(\rho) = -\frac{\hbar^2}{2\mu_\rho}\frac{\partial^2}{\partial \rho^2} + V_{1D}(\rho) \quad (2b)$$

where $V_{1D}(r)$ and $V_{1D}(\rho)$ are the one-dimensional effective potentials for r and ρ coordinates by putting the reaction system in the reactant asymptotic region with other coordinates fixed at the equilibrium geometry.

The split-operator method[38] is employed here to propagate the wavepacket on the PES for the quantum scattering process. The time-dependent wave function can be expanded in terms of the body-fixed rovibrational eigenfuntions defined in terms of the above reactant Jacobi coordinates. After the time-dependent wave function is propagated into the product region, we use the standard time-dependent reactive flux[39−42] method to extract the initial-state-selected reaction probability.

The initial-state-selected integral cross section $\sigma_{\nu_0 j_0}(E)$ is obtained by summing over all of the initial-state-selected reaction probabilities with respect to different partial waves $P^J_{\nu_0 j_0 K_0}(E)$

$$\sigma_{\nu_0 j_0}(E) = \frac{1}{(2j_0+1)}\frac{\pi}{k^2}\sum_J (2J+1)P^J_{\nu_0 j_0 K_0}(E) \quad (3)$$

where $k = (2\mu E)^{1/2}$ and E is the translational energy.

The 4DOF cumulative reaction probability (CRP) is computed by summing over all of the initial-state-selected rovibrational reaction probabilities, $P^{J=0}_{\nu_1\nu_2 j}(E)$[6]

$$N^{J=0}_{4D}(E) = \sum_{\nu_1,\nu_2=0}\sum_{j=0} P^{J=0}_{\nu_1\nu_2 j}(E) \quad (4)$$

In order to directly compare with the experimental rate constants, the energy and J−K shifting methods[44,45] are employed to calculate the theoretical rate constants

$$k(T) = \frac{Q^{\ddagger}_{rot} Q^{\ddagger,(3N-10)}_{vib}}{hQ_r}\int_0^\infty N(E)^{J=0}_{4D} e^{-E/k_B T}\, dE \quad (5)$$

where Q_r is the reactant partition function, which is written as a product of vibrational, rotational, and translational partition functions. $Q^{\ddagger}_{rot}$ is the rigid rotor asymmetric top rotational partition function of the reaction system at the transition state. $Q^{\ddagger,(3N-10)}_{vib}$ is the vibrational partition function with the vibrational frequencies of the transition state that are not explicitly treated in the 4DOF model. E is the total energy in full dimensionality.

3. RESULTS AND DISCUSSION

A. Computational Parameters. For the translational coordinate R, 130 sine basis functions were used to expand the wave function in the range of 3.3−12.3 bohr; among these, 60 functions were chosen to expand the wave function in the interaction region. We used 40 potential-optimized vibrational DVR points[43] for the r coordinate in the range of 0.7−6.5 bohr, 10 potential-optimized vibrational DVR points for CX covering the range of 0.0−2.1 bohr, and 50 spherical harmonic rotational functions for γ. The time-dependent wavepacket was propagated with a time step of 15 au. The above numerical parameters were sufficient to get the initial-state-selected reaction probabilities converged for the current 4DOF reduced-dimensional dynamics study.

B. Vibrational States of CH_4. Initial vibrational states of the reactant CH_4 were obtained by solving the following 2DOF vibrational Schrödinger equation of the pseudotriatom HCX

$$\hat{H}_{HCX}\phi_{\nu_\rho,\nu_r} = E_{\nu_\rho,\nu_r}\phi_{\nu_\rho,\nu_r} \quad (6)$$

where ν_ρ and ν_r represent the vibrational quantum numbers of the stretching vibrations of ρ and r (as seen in Figure 1), respectively. $\hat{H}_{HCX}$ is defined as

$$\hat{H}_{HCX} = h_\rho(\rho) + h_r(r) + V_{2D}(\rho, r) \quad (7)$$

where $h_\rho(\rho)$ and $h_r(r)$ were given in eq 2 and $V_{2D}(\rho,r)$ is the 2DOF potential energy surface at the reactant asymptotic region.

The vibrational levels (ν_ρ,ν_r) of HCX assigned to their corresponding vibrational excitation states are listed in Table 1.

C. Initial-State-Selected Reaction Probabilities. Figure 2 shows the initial-state-selected reaction probabilities for total angular momentum J = 0 for the first eight vibrational initial states of $CH_4(\nu_1,\nu_2)$ as a function of translational energy. First, we notice that the reaction probabilities rise very rapidly as the translational energy increases. For example, as seen for the ground-state reaction probability, the reaction probability rapidly increases about 20 fold from 0.01 to about 0.2 as the translational energy increases from 0.01 to 0.2 eV. The increase reaches to ∼26 fold at 0.38 eV. Thus, the translational energy greatly enhances the reactivities for translational energy less than 0.38 eV. However, the reaction probability stays almost constant after 0.38 eV for the ground state, which means that

dx.doi.org/10.1021/jp4005778 | J. Phys. Chem. A 2013, 117, 7124−7130

Table 1. Initial Vibrational States, (ν_ρ,ν_r), of $CHX(H_3)$[a]

state no.	(ν_ρ,ν_r)	E_a (cm^{-1})	E (cm^{-1})
1	(0,0)	2254	0
2	(0,1)	3680	1425
3	(0,2)	5105	2851
4	(1,0)	5235	2981
5	(0,3)	6551	4297
6	(1,1)	6645	4390
7	(0,4)	8033	5779
8	(1,2)	8083	5829
9	(2,0)	8104	5850

[a]The energy levels E_a and E are relative to the FCH_4 asymptotic region and the ground vibrational state, respectively.

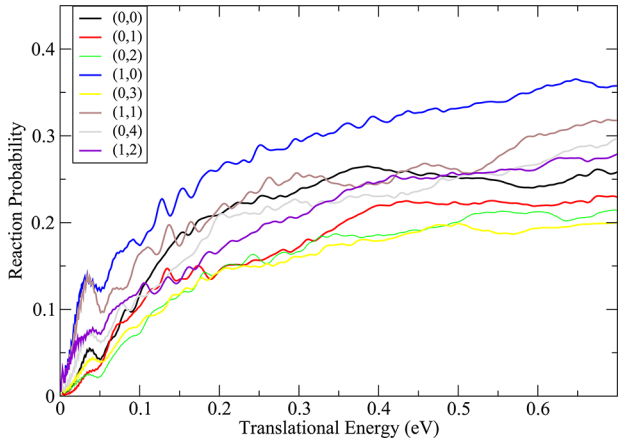

Figure 2. Initial state-selected reaction probabilities for F + $CH_4(\nu_\rho,\nu_r)$ as a function of translational energy with $j = 0$ and $J = 0$.

the translation energy does not have a significant effect on the reactivity for energies greater than 0.38 eV.

As the vibrational quantum numbers increase, the C−X(r) vibration does not enhance the reaction probability; instead, it hinders the reactivity as the (0,1), (0,2), (0,3), and (0,4) reaction probabilities are all lower than the ground-state reaction probability. Nonetheless, the stretching motion of C−H(ρ) enhances the reaction probability as the (1,0) reaction probability is greater than that of the ground state. However, the average increase of the reaction probability from (0,0) to (1,0) is only about a factor of 1.3. On the basis of the above results, we can conclude that the translational energy is more effective on the reactivity below 0.38 eV than the vibrational energy for this polyatomic reaction. However, the vibrational energy is more effective on the reactivity than the translational energies higher than 0.38 eV.

Second, this potential energy surface has a very small barrier of around ~0.02 eV (the best ab initio prediction including spin−orbit effects is 0.03 eV).[2] Because the reaction probability shows up below 0.02 eV, for example, for the (1,0) state, the reaction probability even reaches about 0.1 at 0.02 eV, the tunneling effect seems to be prominent for this reaction. This is expected because a light atom (H) is abstracted from HCX to form HF with the F atom.

Third, all of the vibrational-mode-selective reaction probability curves show resonance peaks. Furthermore, all of the resonance peaks appear at around 0.04 eV just after the reaction threshold. The resonance feature showing up close to the reaction threshold was observed in the F + CH_4 experiment by Liu et al.[17,18]

In general, on the basis of the vibrational-state-selective reaction probabilities, we can conclude that with an early barrier in the reactant channel, the translational energy greatly enhances the reactivity for translational energy below 0.38 eV; however, it has less effect than the vibrational energy at higher energies. In addition, the C−H stretching motion only slightly affects the reaction, whereas the umbrella motion hinders the reactivity. Furthermore, all of the reaction probabilities show a common resonance peak just after the threshold energy at around 0.04 eV, which confirms the experimental finding of resonance in this reaction.

D. Integral Cross Section. In order to calculate the integral cross section, all reaction probabilities for different partial waves up to $J = 135$ are calculated to converge the translational energy up to 0.7 eV. Figure 3 shows the plot of the reaction probability

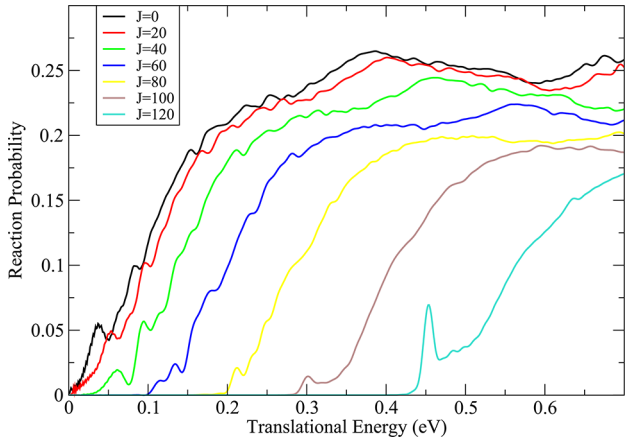

Figure 3. Reaction probability for different partial waves $J = 0$, 20, 40, 60, 80, 100, and 120 as a function of translation energy.

for seven different partial waves, $J = 0$, 20, 40, 60, 80, 100, and 120. Note that the common resonance peak after the threshold, found in the $J = 0$ computations, shows up in every partial wave ($J > 0$) reaction probability. Using eq 3, the integral cross section for the ground-state reaction is plotted in Figure 4. Because each H atom in CH_4 should have an equal opportunity to react, the integral cross section is multiplied by a factor of 4 for the ground vibrational state before plotted in Figure 4. In

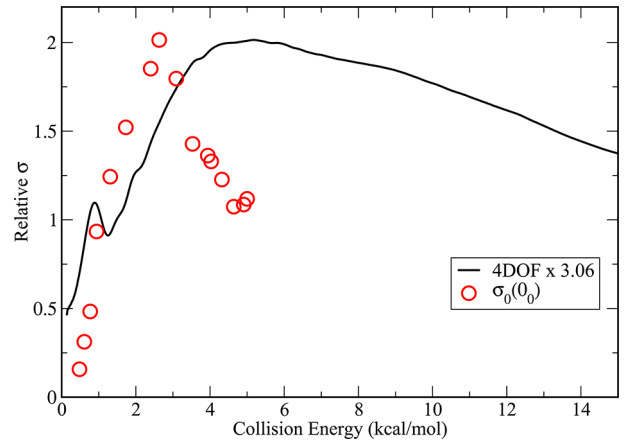

Figure 4. Comparison of the 4DOF integral cross section for the ground-state F + $CH_4(\nu_\rho = 0,\nu_r = 0)$ reaction with the experimental excitation function.[34]

dx.doi.org/10.1021/jp4005778 | J. Phys. Chem. A 2013, 117, 7124−7130

Figure 4, we also compare our ground-state integral cross sections, obtained by summing over all of the product states, with the most recent measurement of the excitation functions by Liu et. al.[34] Because the experiment did not report absolute cross sections, we rescaled the computed excitation function by a factor of 3.06 in order to help the comparison between the measured and computed data. Both the calculated and measured excitation functions have a steep rise after the threshold, but the experimental excitation function peaks at around 2.6 kcal/mol, whereas the computed peak occurs at about 5.1 kcal/mol. Furthermore, the decrease in the measured cross section after the peak is much steeper than that in the calculations. The above differences may be explained as follows. First, and perhaps most importantly, the measured excitation function, $\sigma_0(0_0)$ in Figure 8 of ref 34 corresponds to the F + $CH_4(\nu = 0) \rightarrow$ HF + $CH_3(\nu = 0)$ reaction. The $\sigma_0(1_1)$ cross sections, which are also measured and correspond to the ground-state reactant and the symmetric-stretch excited product $CH_3(\nu_1 = 1)$, are virtually negligible. However, the umbrella-excited $CH_3(\nu_2 = 1,2,...)$ products are not reported in ref 34, which may also have significant populations, especially at higher collision energies; thus, $\sigma_0(0_0)$ underestimates the total cross sections and shows a faster decay as the collision energy increases. Second, in the present model, there are no internal rotational motions included for CH_4 except the external rotational motion of the F atom with respect to the CH_4 center of mass rotation. As a result, during the collision process, the vibrational energy of CH_4 cannot be efficiently transferred to the rotational motions and to the other neglected vibrational DOFs, which makes the CH vibration more active than that in reality (experiment); thus, theory shows a later peak and slower decay of the cross sections after the position of the peak. Third, experiment may underestimate the cross sections at higher collision energies because experiment only probes the low-N states of the CH_3 products, which warrants caution when comparing theory and experiment, as was shown recently for the Cl + CHD_3 reaction.[8]

Figure 4 also shows that even after the averaging over the different partial waves, a prominent resonance peak still appears at 0.038 eV, which is just after the reaction threshold. This confirms the experimental finding of Liu et al.[18,19] that the resonances can survive the averaging over impact parameters and show up in the integral cross sections.

There is also another measurement on the absolute integral cross sections by Aquilanti et al.[21] for the title reaction. However, the experiment did not sample the regions of the PES directly leading to reaction because the measured integral cross sections were mostly dominated by large impact parameters. Another issue why we cannot compare this experiment to the present state-specific 4DOF results is that the cross sections were measured for the sum of all of the reactant and product states.

We notice that the 5DOF F + CH_4 study by Han et al.,[27] based on the two semiempirical PESs, found the resonance close to the threshold on one of the PESs, but the resonance feature disappeared for partial waves $J > 30$, and the two integral cross sections on the two PESs had totally different shapes, and only one of them showed a very broad resonance feature at around 0.06 eV. On their second 5DOF study on the semiempirical PES-2006,[29] a single resonance peak was found in the reaction probabilities for $J \leq 55$. They did not find a resonance peak on the ground-state integral cross section but found a resonance peak, at 0.015 eV, for the integral cross section of the first excited umbrella motion. The 3DOF study by Nyman et al.[28] also on the PES-2006 shows resonance features, one at ~0.06 eV and another at ~0.13 eV on the ground-state integral cross section. Note that all of the integral cross sections from the above three dynamics calculations show a gradual increase as the energy increases. This is different from the present ground-state integral cross section. Our integral cross section shows a rapid increase from 0.01 to 0.2 eV, and then, it decreases as the energy increases. This behavior is also found in the experimental cross section by Liu et al.,[18,34] that is, the integral cross section rapidly increases from the threshold to reach a maximum at ~0.1 eV and then decreases as the energy increases. However, as mentioned earlier, the experimental integral cross section is specific for the $CH_3(\nu = 0)$ product state, whereas our calculation gives the total integral cross section involving all of the product states. Thus, we cannot directly compare our results with experiment. The current study shows that the resonance peak appears in every partial wave reaction probability; this is different from the previous calculations too. We think that the major differences on the integral cross section and partial waves in the above quantum dynamics calculations are mainly due to the characters and accuracies of the different PESs used in these dynamics studies.

E. Cumulative Reaction Probability and Rate Constant. The 4DOF cumulative reaction probability is obtained by summing over all of the rovibrational states of CH_4. In order to converge the translational energy up to 0.5 eV, rotational states up to a maximum j of 10, 7, 4, and 3 are computed for the (0,0), (0,1), (0,2), and (1,0) vibrational states, respectively. In Figure 5, the reaction probabilities for the reactant ground

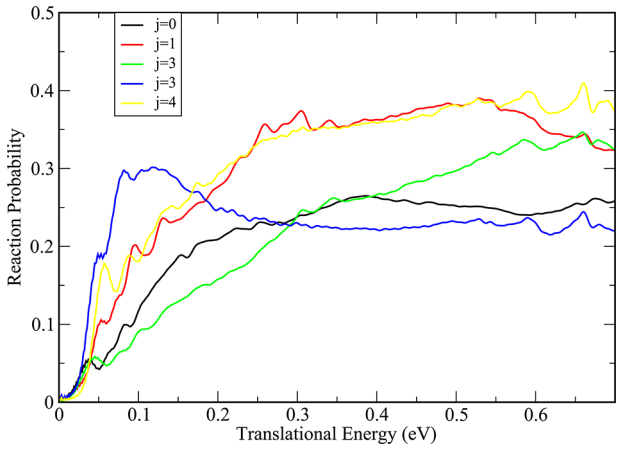

Figure 5. Rotational dependence of the reaction probabilities for F + $CH_4(\nu_\rho = \nu_r = 0,j)$ as a function of translational energy with $J = 0$.

and first four rotational excitation states are shown. By summing over all of the rovibrational states of CH_4, the 4DOF reduced-dimensional cumulative reaction probability is obtained, as shown in Figure 6.

In eq 5, the rotational constant to calculate the reactant rotational partition function is 5.27 cm^{-1}. At the bent transition state, F−CH_4 is an asymmetric top, and the three rotational constants are 5.44, 0.27, and 0.26 cm^{-1} for the $Q^{\ddagger}_{rot}$ calculation. For the reactant vibrational partition function, the harmonic vibrational frequencies[2] are used. There are eight vibrational frequencies "missing" from our 4DOF reduced-dimensional calculation at the transition state, which are 40, 1335, 1361, 1520, 1539, 3070, 3185, and 3203 cm^{-1}. They are used to

dx.doi.org/10.1021/jp4005778 | J. Phys. Chem. A 2013, 117, 7124−7130

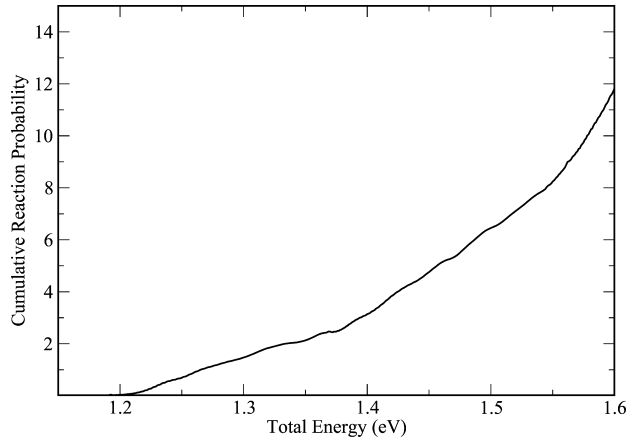

Figure 6. The 4DOF reduced-dimensional cumulative reaction probability as a function of total energy.

compute the vibrational partition function at the transition state, $Q_{vib}^{\ddagger(3N-10)}$.

In Figure 7, we compare our theoretical results with two experimental $k(T)$ for the F + CH_4 reaction. Until today, there

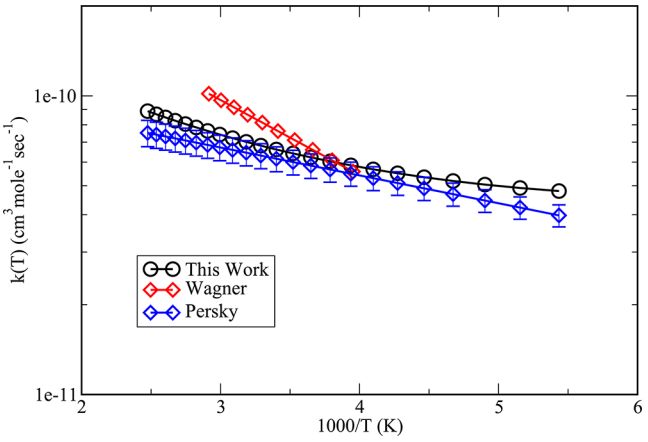

Figure 7. Comparison of the rate constants between the present 4DOF quantum dynamics results and two experimental results of Wagner et al.[37] and Persky.[20].

have been three experimental reports that directly determined the rate constants as a function of temperature.[20,37,46] However, only Persky's[20] (from 184 to 406 K) and Wagner's[37] results (from 253 to 352 K) have a linear dependency on the temperature, and the $k(T)$ from Moore et al.[46] exhibits a very unusual temperature dependence. Therefore, here, only Persky's and Wagner's results have been plotted against our computed ones from 184 to 406 K in Figure 7. Note that the two measurements show quite different slopes of the rate curves. Nonetheless, our theoretical results on the present ab initio PES, in general, agree well with Persky's results, and at the lower- and higher-temperature ends, our results are slightly bigger than Persky's results.

4. CONCLUSIONS

We have carried out reduced-dimensional quantum reaction dynamics, time-dependent wavepacket propagation computations to study the F + $CH_4(v,j)$ → HF + CH_3 reaction. A four degree-of-freedom approach is employed to study the initial-state-selective reaction probabilities, reactive resonances, and rate constants on the slightly modified version of the full-dimensional ab-initio-based PES reported in ref 2.

The initial-state-selected reaction probability is reported in this paper for total angular momentum $J = 0$. We observe a common resonance peak showing up on the reaction probabilities near the reaction threshold for all of the vibrational states. Our study shows that the vibrational excitation of C−H has less effect on the reactivity than translational energy, and the vibrational umbrella motion of C−H_3 hinders the reactivity. The calculations also show that the translational energy enhances the reactivity more than the vibrational energy for energies less than 0.38 eV, and the reverse is true for energies higher than 0.38 eV. The resonance feature shows up in the initial-state-selected reaction probabilities and also appears on the integral cross section spectrum. This confirms the experimental detection of the resonance feature of this reaction.[17,18] The comparison of the rate constants between our theoretical calculations and direct experiment measurements shows that our results agree with Persky's results well.

In addition, the current study indicates that for polyatomic reactions, due to the complexity of the PES, it is difficult to predict which driving force is the more effective one to activate the reaction. Nevertheless, we hope that more and more research on polyatomic reactions will uncover the fundamental rules of complex chemical processes.

■ ASSOCIATED CONTENT

Supporting Information

Properties (structures and relative energies of the stationary points) of the modified version of the full-dimensional ab initio potential energy surface. This material is available free of charge via the Internet at http://pubs.acs.org.

■ AUTHOR INFORMATION

Corresponding Author

*E-mail: dywang@sdnu.edu.cn.

Notes

The authors declare no competing financial interest.

†E-mail: czako@chem.elte.hu

■ ACKNOWLEDGMENTS

The authors thank Dr. Kopin Liu for sending the experimental excitation function. D.Y.W. thanks the Tanshan Scholarship Funds of Shandong Province and the National Science Funding of China (Grant No. 10944006) for supporting this work. G.C. would like to acknowledge the Scientific Research Fund of Hungary (OTKA, NK83583) and the Magyary Fellowship of the European Union and Hungary (TÁMOP 4.2.4.A/1-11-1-2012-0001) for financial support.

■ REFERENCES

(1) Polanyi, J. C. Some Concepts in Reaction Dynamics. *Science* **1987**, *236*, 680−690.

(2) Czakó, G.; Shepler, B. C.; Braams, B. J.; Bowman, J. M. Accurate Ab Initio Potential Energy Surface, Dynamics, and Thermochemistry of the F + CH_4 → HF + CH_3 Reaction. *J. Chem. Phys.* **2009**, *130*, 084301.

(3) Xie, Z.; Braams, B. J.; Bowman, J. M. Ab Initio Global Potential-Energy Surface for H_5^+ → H_3^+ + H_2. *J. Chem. Phys.* **2005**, *122*, 224307.

(4) Wang, D. Y.; Xie, Z.; Bowman, J. M. Seven-Degree-of-Freedom, Quantum Scattering Dynamics Study of the H_2D^+ + H_2 Reaction. *J. Chem. Phys.* **2010**, *132*, 084305.

(5) Yan, S.; Wu, Y.-T.; Zhang, B.; Yue, X.-F.; Liu, K. Do Vibrational Excitations of CHD_3 Preferentially Promote Reactivity Toward the Chlorine Atom? *Science* **2007**, *316*, 1723−1726.
(6) Meng, F. B; Yan, W.; Wang, D. Y. Quantum Dynamics Study of the Cl + CH_4 → HCl +CH_3 Reaction: Reactive Resonance, Vibrational Excitation Reactivity, and Rate Constants. *Phys. Chem. Chem. Phys.* **2012**, *14*, 13656−13662.
(7) Zhang, Z.; Zhou, Y.; Zhang, D. H.; Czakó, G.; Bowman, J. M. Theoretical Study of the Validity of the Polanyi Rules for the Late-Barrier Cl + CHD_3 Reaction. *J. Phys. Chem. Lett.* **2012**, *3*, 3416−3419.
(8) Wang, F.; Lin, J.-S.; Cheng, Y.; Liu, K. Vibrational Enhancement Factor of the Cl + $CHD_3(\nu_1=1)$ Reaction: Rotational-Probe Effects. *J. Phys. Chem. Lett.* **2013**, *4*, 323−327.
(9) Czakó, G.; Bowman, J. M. Dynamics of the Reaction of Methane with Chlorine Atom on an Accurate Potential Energy Surface. *Science* **2011**, *334*, 343−346.
(10) Persky, A. Kinetics of the F + CH_4 Reaction in the Temperature Range 184−406 K. *J. Phys. Chem.* **1996**, *100*, 689−693.
(11) (a) Persky, A. Kinetics of the Reactions F + H_2S and F + D_2S at 298 K. *Chem. Phys. Lett.* **1998**, *298*, 390−394. (b) Erratum: Persky, A. Kinetics of the Reactions F + H_2S and F + D_2S at 298 K. *Chem. Phys. Lett.* **1999**, *306*, 416.
(12) Nazar, M. A.; Polanyi, J. C. Energy Distribution among Reaction Products. XIV. F + CH_4, F + CH_3X(X=Cl,Br,I), F + CH_nCl_{4n} (n=1−3). *Chem. Phys.* **1981**, *55*, 299−311.
(13) Wickramaaratchi, M. A.; Setser, D. W.; Hildebrandt, H.; Korbitzer, B.; Heydtmann, H. Evaluation of HF Product Distributions Deduced from Infrared Chemiluminiscence. II. F Atom Reactions. *Chem. Phys.* **1985**, *94*, 109−129.
(14) Maneshkarimi, M.; Heydtmann, H. Infrared Chemiluminescence in a Mixed Reaction Situation: F + CH_4 and F + $CHCl_3$. *Can. J. Chem.* **1994**, *72*, 790−794.
(15) Harper, W. W.; Nizkorodov, S. A.; Nesbitt, D. Quantum State-Resolved Reactive Scattering of F + CH_4 → HF(ν,J) + CH_3: Nascent HF(ν,J) Product State Distributions. *J. Chem. Phys.* **2000**, *113*, 3670−3680.
(16) Zhou, J.; Lin, J. J.; Shiu, W.; Pu, S. C.; Liu, K. Crossed-Beam Scattering of F + CD_4 → DF + $CD_3(\nu$NK): The Integral Cross Sections. *J. Chem. Phys.* **2003**, *119*, 2538−2544.
(17) Shiu, W.; Lin, J. J.; Liu, K.; Wu, M.; Parker, D. H. Imaging the Pair-Correlated Excitation Function: The F + CH_4 → HF(ν') + $CH_3(\nu = 0)$ Reaction. *J. Chem. Phys.* **2004**, *120*, 117−122.
(18) Shiu, W.; Lin, J. J.; Liu, K. Reactive Resonance in a Polyatomic Reaction. *Phys. Rev. Lett.* **2004**, *92*, 103201.
(19) Zhou, J.; Lin, J. J.; Liu, K. Observation of a Reactive Resonance in the Integral Cross Section of a Six-Atom Reaction: F + CHD_3. *J. Chem. Phys.* **2004**, *121*, 813−818.
(20) Persky, A. The Temperature Dependence of the Kinetic Isotope Effect in the Reaction of F Atoms with CH_4 and CD_4. *Chem. Phys. Lett.* **2006**, *430*, 251−254.
(21) Aquilanti, V.; Candori, R.; Cappelletti, D.; Luzzatti, E.; Pirani, F. Scattering of Magnetically Analyzed F(^2P) Atoms and Their Interactions with He, Ne, H_2 and CH_4. *Chem. Phys.* **1990**, *145*, 293−305.
(22) Corchado, J. C.; Espinosa-Garcia, J. Theoretical Study of the CH_4 + F → CH_3 + FH Reaction. II. Semiempirical Surfaces. *J. Chem. Phys.* **1996**, *105*, 3160−3167.
(23) Troya, D.; Milan, J.; Banos, I.; Gonzalez, M. Ab Initio Potential Energy Surface, Variational Transition State Theory, and Quasiclassical Trajectory Studies of the F + CH_4 → HF + CH_3 Reaction. *J. Chem. Phys.* **2004**, *120*, 5181−5191.
(24) Roberto-Neto, O.; Machado, F. B. C.; Ornellas, F. R. Dual-Level Direct Dynamics Calculations of Kinetic Isotope Effects for the CH_4 + F → CH_3 + HF Abstraction Reaction. *Chem. Phys. Lett.* **2005**, *409*, 38−42.
(25) Rangel, C.; Navarrete, M.; Espinosa-Garcia, J. Potential Energy Surface for the F($^2P_{3/2}$,$^2P_{1/2}$) + CH_4 Hydrogen Abstraction Reaction. Kinetics and Dynamics Study. *J. Phys. Chem. A* **2005**, *109*, 1441−1448.
(26) Castillo, J. F.; Aoiz, F. J.; Banares, L.; Martinez-Nunez, E.; Fernandez-Ramos, A.; Vazquez, S. Quasiclassical Trajectory Study of the F + CH_4 Reaction Dynamics on a Dual-Level Interpolated Potential Energy Surface. *J. Phys. Chem. A* **2005**, *109*, 8459−8470.
(27) Chu, T.; Zhang, X.; Ju, L.; Yao, L.; Han, K.-L.; Wang, M.; Zhang, J. Z. H. First Principles Quantum Dynamics Study Reveals Subtle Resonance in Polyatomic Reaction: The Case of F + CH_4 → HF + CH_3. *Chem. Phys. Lett.* **2006**, *242*, 243−246.
(28) Nyman, G.; Espinosa-Garcia, J. Reduced Dimensionality Quantum Scattering Calculations on the F + CH_4 → FH + CH_3 Reaction. *J. Phys. Chem. A* **2004**, *111*, 11943−11947.
(29) Chu, T.; Han, K.; Espinosa-Garcia, J. A Five-Dimensional Quantum Dynamics Study of the F(^2P) + CH_4 Reaction. *J. Chem. Phys.* **2009**, *131*, 244303.
(30) von Horsten, H. F.; Clary, D. C. Reactive Resonances in the F + CHD_3 Reaction—A Quantum-Dynamics Study. *Phys. Chem. Chem. Phys.* **2011**, *13*, 4340−4356.
(31) Czakó, G.; Bowman, J. M. CH Stretching Excitation Steers the F Atom to the CD Bond in the F + CHD_3 Reaction. *J. Am. Chem. Soc.* **2009**, *131*, 17534−17535.
(32) Czakó, G.; Bowman, J. M. Quasiclassical Trajectory Calculations of Correlated Product Distributions for the F + $CHD_3(\nu_1$ = 0,1) Reactions Using an Ab Initio Potential Energy Surface. *J. Chem. Phys.* **2009**, *131*, 244302.
(33) Zhang, W.; Kawamata, H.; Liu, K. CH Stretching Excitation in the Early Barrier F + CHD_3 Reaction Inhibits CH Bond Cleavage. *Science* **2009**, *325*, 303−306.
(34) Kawamata, H.; Zhang, W.; Liu, K. Imaging the Effects of the Antisymmetric Stretch Excitation of CH_4 in the Reaction with F Atom. *Faraday Discuss.* **2012**, *157*, 89−100.
(35) Jordan, M. J. T.; Gilbert, R. G. Classical Trajectory Studies of the Reaction CH_4 + H → CH_3 + H_2. *J. Chem. Phys.* **1995**, *102*, 5669−5683.
(36) Espinosa-Garcia, J.; Bravo, J. L.; Rangel, C. New Analytical Potential Energy Surface for the F(^{2}P) + CH_4 Hydrogen Abstraction Reaction: Kinetics and Dynamics. *J. Phys. Chem. A* **2007**, *111*, 2761−2771.
(37) Wagner, H. Gg.; Warnatz, J.; Zetzch, C. Reaction of Fluorine Atoms with Methane. *An. Asoc. Quim. Argent.* **1971**, *59*, 169−177.
(38) Fleck, J. A., Jr.; Morris, J. R.; Feit, J. R. Time-Dependent Propagation of High Energy Laser Beams through the Atmosphere. *Appl. Phys.* **1976**, *10*, 129−160.
(39) Zhang, D. H.; Zhang, J. H. Z. Full-Dimensional Time-Dependent Treatment for Diatomdiatom Reactions: The H_2 + OH Reaction. *J. Chem. Phys.* **1994**, *101*, 1146−1156.
(40) Zhang, D. H.; Zhang, J. H. Z. Quantum Reactive Scattering with a Deep Well: Time-Dependent Calculation for H + O_2 Reaction and Bound State Characterization for HO_2. *J. Chem. Phys.* **1994**, *101*, 3671−3678.
(41) Wang, D. Y. An Eight-Degree-of-Freedom Quantum Dynamics Study for the H_2 + C_2H System. *J. Chem. Phys.* **2005**, *123*, 194302.
(42) Wang, D. Y.; Huo, W. M. An Eight-Degree-of-Freedom Quantum Dynamics Study of the Isotopic Effect on the Reaction: HD + C_2H. *J. Chem. Phys.* **2008**, *129*, 084303.
(43) Echave, J.; Clary, D. C. Potential Optimized Discrete Variable Representation. *Chem. Phys. Lett.* **1992**, *190*, 225−230.
(44) Bowman, J. M. Reduced Dimensionality Theory of Quantum Reactive Scattering. *J. Phys. Chem.* **1991**, *95*, 4960−4968.
(45) Bowman, J. M.; Wagner, A. F. In *The Theory of Chemical Reaction Dynamics*; Clary, D. C., Ed.; Reidel: Dordrecht, The Netherlands, 1986.
(46) Moore, C. M.; Smith, I. W. M.; Stweart, D. W. A. Rates of Processes Initiated by Pulsed Laser Production of F Atoms in the Presence of HCl, CH_4, and CF_3H. *Int. J. Kinet.* **1996**, *26*, 813−825.